



## Article

# Mixture of Sludge and Chicken Manure in Membrane-Less Microbial Fuel Cell for Simultaneous Waste Treatment and Energy Recovery

Nurul Najwa Adam Malik <sup>1</sup>, Muhammad Najib Ikmal Mohd Sabri <sup>1</sup>, Husnul Azan Tajarudin <sup>1</sup> ,  
Noor Fazliani Shoparwe <sup>2</sup> , Hafiza Shukor <sup>3</sup>, Muaz Mohd Zaini Makhtar <sup>1,4,\*</sup>, Syed Zaghum Abbas <sup>5</sup>,  
Yang-Chun Yong <sup>5</sup> and Mohd Rafatullah <sup>6,\*</sup> 

<sup>1</sup> Bioprocess Technology Division, School of Industrial Technology, Universiti Sains Malaysia, Penang 11800, Malaysia; najwaadam@student.usm.my (N.N.A.M.); najibikmalmohdsabri@student.usm.my (M.N.I.M.S.); azan@usm.my (H.A.T.)

<sup>2</sup> Faculty of Bioengineering and Technology, Universiti Malaysia Kelantan, Jeli 17600, Malaysia; fazliani.s@umk.edu.my

<sup>3</sup> Centre of Excellence for Biomass Utilization, Faculty of Chemical Engineering Technology, Universiti Malaysia Perlis, Arau 02600, Malaysia; hafizashukor@unimap.edu.my

<sup>4</sup> Centre for Global Sustainability Studies, Universiti Sains Malaysia, Penang 11800, Malaysia

<sup>5</sup> Biofuels Institute, School of Environment and Safety Engineering, Jiangsu University, Zhenjiang 212013, China; zabbas@ujs.edu.cn (S.Z.A.); ycyong@ujs.edu.cn (Y.-C.Y.)

<sup>6</sup> Environmental Technology Division, School of Industrial Technology, Universiti Sains Malaysia, Penang 11800, Malaysia

\* Correspondence: muazzaini@usm.my (M.M.Z.M.); mrafatullah@usm.my (M.R.)



**Citation:** Malik, N.N.A.; Sabri, M.N.I.M.; Tajarudin, H.A.; Shoparwe, N.F.; Shukor, H.; Makhtar, M.M.Z.; Abbas, S.Z.; Yong, Y.-C.; Rafatullah, M. Mixture of Sludge and Chicken Manure in Membrane-Less Microbial Fuel Cell for Simultaneous Waste Treatment and Energy Recovery. *Catalysts* **2022**, *12*, 776. <https://doi.org/10.3390/catal12070776>

Academic Editor: Barbara Mecheri

Received: 26 April 2022

Accepted: 30 June 2022

Published: 13 July 2022

**Publisher's Note:** MDPI stays neutral with regard to jurisdictional claims in published maps and institutional affiliations.



**Copyright:** © 2022 by the authors. Licensee MDPI, Basel, Switzerland. This article is an open access article distributed under the terms and conditions of the Creative Commons Attribution (CC BY) license (<https://creativecommons.org/licenses/by/4.0/>).

**Abstract:** In addition to disposal issues, the abundance of sludge and chicken manure has been a rising issue in Malaysia. Membrane-less microbial fuel cell (ML-MFC) technology can be considered as one of the potential solutions to the issues of disposal and electricity generation. However, there is still a lack of information on the performance of an ML-MFC powered by sludge and chicken manure. Hence, with this project, we studied the performance of an ML-MFC supplemented with sludge and chicken manure, and its operating parameters were optimized using response surface methodology (RSM) through central composite design (CCD). The optimum operating parameters were determined to be 35 °C, 75% moisture content, and an electrode distance of 3 cm. Correspondingly, the highest power density, COD removal efficiency, and biomass acquired through this study were 47.2064 mW/m<sup>2</sup>, 98.0636%, and 19.6730 mg/L, respectively. The obtained COD values for dewatered sludge and chicken manure were 708 mg/L and 571 mg/L, respectively. COD values were utilized as a standard value for the substrate degradation by *Bacillus subtilis* in the ML-MFC. Through proximate analyses conducted by elemental analysis and atomic absorption spectrometry (AAS), the composition of carbon and magnesium for sludge and chicken manure was 23.75% and 34.20% and 78.1575 mg/L and 71.6098 mg/L, respectively. The proposed optimal RSM parameters were assessed and validated to determine the ML-MFC operating parameters to be optimized by RSM (CCD).

**Keywords:** membrane-less microbial fuel cell; solid waste; sludge; chicken manure; renewable energy; operating parameters; electricity; sustainable development goals

## 1. Introduction

The simple definition of energy is the ability to do work that can neither be created nor destroyed. There are various forms of energy, including chemical energy, potential energy, and kinetic energy [1]. These various types of energy are often utilized in combination to generate a desired output, such as heat or electricity. Energy resources can be classified into

three categories: fossil fuels, nuclear energy, and renewable resources [2]. Depending on the source, energy can be broadly classified as renewable or non-renewable.

There is currently an increasing global demand for electricity as a result of widespread industrialization. Recent extensive exploration of innovative forms of energy conversion in various industrial sectors has contributed to the increase in energy consumption and demand [1]. This pattern has been observed in Malaysia; Haiges et al. (2017) reported that Malaysia's electricity demand growth rates have been increased annually since 2013 [3].

Many countries that have been heavily dependent on fossil fuels, which are commonly categorized as non-renewable energy resources. Aside from its notable negative impact on the environment, such as its considerable contribution to global warming because of its ever-increasing emissions of greenhouse gases, the use of fossil fuels is also associated with issues related to the rapid depletion of natural resources, lack of energy security, and steady price increases.

Malaysia is a country with monsoon winds climate with relatively high temperatures and humidity levels [4]. This could be the reason that solar and wind energy cannot be efficiently harvested. In addition to the contribution of solar and wind energy to power generation in Malaysia, biomass has the potential to supply as much as 3% of total power production in the country [5]. To this end, abundant of agricultural and animal husbandry waste could be used in combination with microbial fuel cell (MFC) technology.

The poultry industry is a major contributor to Malaysia's GDP due to the high consumption rate of poultry products in the country. It was forecasted that Malaysia would be one of the world's top poultry consumers in the year 2020, with an estimated consumption of 49.4 kg poultry meat per person [6]. This forecast is close to Malaysia's actual poultry consumption per capita in 2019 of 49 kg [6]. Due to the large amount of chicken manure secreted daily as a consequence of the high poultry population in the country, the industry has faced issues with respect to its disposal methods, leading to environmental issues, as well as odor pollution. The high concentration of ammonia (20 ppm) in chicken manure also has negative effects on chickens [7].

Similarly, the abundance of sludge is another issue of increasing importance in Malaysia; the volume of sludge production in Malaysia has increased in recent years, with three million metric tons of sewage sludge generated annually [8]. This rate of sludge production was predicted to increase to seven million metric tons in 2020 [8] due to factors such as industrialization and increased human population. Similarly, to the abundance of chicken manure, the abundance of sludge production in Malaysia is met with disposal and environmental issues, both of which have led to an increase in waste management costs. Despite the issue of the abundance of both sludge and chicken manure in Malaysia, there is still a lack in its utilization, particularly as a feedstock. Both sludge and chicken manure are associated with high levels of unrecovered energy, hence; therefore, we decided to mix the two as a feedstock in this study.

There is currently a lack of information on the combination of dewatered sludge and chicken manure as feedstock in MFCs, despite their prevalence in this field of study. This is because a majority of studies conducted on dewatered sludge consider either sludge alone or as part of a mixture with other substrates [9]. Furthermore, future prospects of such combinations are pertinent, as various studies have reported that substrates complementing each other when combined. Jaeel (2015) [10] reported that mixed feedstock facilitates improved utilization of complex carbon sources as a consequence of a more extensive substrate acceptability due to the presence of different bacterial species. The addition of chicken manure to dewatered sludge was reported by El-Nahhal (2020) and Zahedi (2020) [9,11] to have the potential to increase carbon sources in feedstock, effectively facilitating improved degradation by bacteria. Therefore, a study on dewatered sludge and chicken manure as a mixed feedstock is imperative to maximize the potential of substrates in MFCs.

There is a lack of information on the optimization of response surface methodology (RSM) via central composite design (CCD) for electricity generation with membrane-less

MFC (ML-MFC) using sludge and chicken manure as substrates. ML-MFC is a configuration that can be implemented without the use of a membrane, instead using the substrates as a pseudo-membrane. The membrane itself comprised of chemical substances and can be costly. For instance, the substrate is used by bacteria, transferring electrons through electrodes. There is a lack of studies using CCD on such substrates, despite the relatively sufficient number of studies already having been conducted on electricity generation via MFC. Most studies conducted on electricity generation via ML-MFC have been focused on glucose as the carbon source, as opposed to waste being used as the carbon source for the system. Furthermore, most optimization-based studies have been focused on a single substrate instead of a combination of substrates.

Therefore, membrane-less microbial fuel cells (ML-MFCs) can be considered a possible solution, representing a renewable energy technology, as a bioelectrochemical system that produces energy using micro-organisms [12]. Various waste substrates that are generated throughout Malaysia can be collected to this end. We therefore selected chicken manure and dewatered sludge as substrates to be implemented in an ML-MFC. Such a dual substrate could enhance electricity generation.

## 2. Results and Discussion

### 2.1. Proximate Analysis of Substrates

A proximate analysis was conducted in this study to identify and characterize the composition of the substrates. It is important to conduct an analysis to determine the substrate's suitability and usefulness with respect to the ML-MFC's performance [13]. Substrate composition was analyzed by atomic absorption spectroscopy (AAS), elemental analysis, and inductively coupled plasma optical emission spectroscopy (ICP-OES). Through an analysis with an elemental analyzer, carbon (C) was found to yield the greatest composition amongst the macronutrients for both dewatered sludge and chicken manure at 23.75% and 34.20%, respectively (Table 1). Hydrogen accounted for 3.45% of the composition of dewatered sludge compared to chicken manure, with 3.88%. Dewatered sludge was composed of 3.27% nitrogen compared to 4.5% nitrogen content in chicken manure. Magnesium was observed to have the highest content amongst the micronutrients in both dewatered sludge and chicken manure at 78.1575 mg/L and 71.6098 mg/L, respectively. The most abundant trace element in dewatered sludge was determined to be manganese, whereas that in chicken manure was iron. AAS analysis revealed a negative cadmium concentration in chicken manure, which means that there is no cadmium present in the substrate. Trace elements are required by bacteria to carry out metabolic reactions, chemical synthesis, and power generation (protons). Trace elements, such as metal ions, are capable of acting as cofactors and therefore aiding bacteria in their enzymatic reactions [14]. This is important to ensure that enzymatic reactions are completed and vital enzymes are secreted by the bacteria. Enzymes are considered important for the performance of ML-MFCs, as they are responsible for degrading the substrates into simpler components. However, it is worth noting that trace elements are only required in relatively small doses, as excessive doses of such elements could inhibit enzyme generation. Therefore, both dewatered sludge and chicken manure have the potential to be used as feedstock for EB growth in ML-MFCs with the goal of electricity generation.

**Table 1.** Proximate analyses of dewatered sludge and chicken manure.

Type	Trace Element	Unit	Dewatered Sludge	Chicken Manure
Macronutrient	Carbon		23.7500	34.2000
	Nitrogen	%	3.2700	4.5000
	Hydrogen		3.4500	3.8800
Micronutrient	Magnesium	mg/L	78.1575	71.6098
	Zinc		33.2326	4.6382
Trace elements	Iron	mg/L	0.0050	9.7642
	Manganese		5.3913	5.4152
	Cadmium		0.0050	1.7000
Chemical oxygen demand	Organic carbon	mg/L	708.0000	571.0000

## 2.2. Statistical Experimental Design

### 2.2.1. Optimization of Electricity Generation by Response Surface Methodology (RSM) via Central Composite Design (CCD)

A statistical tool, response surface methodology (RSM) via CCD, was utilized in this project to further study the relationship of three [3] independent variables (distance between electrodes (A), moisture content (B), and temperature (C)) with three responses (biomass (Y1), COD removal efficiency (Y2), and power density (Y3)).

#### Development of the Regression Model Equation and Statistical Analysis

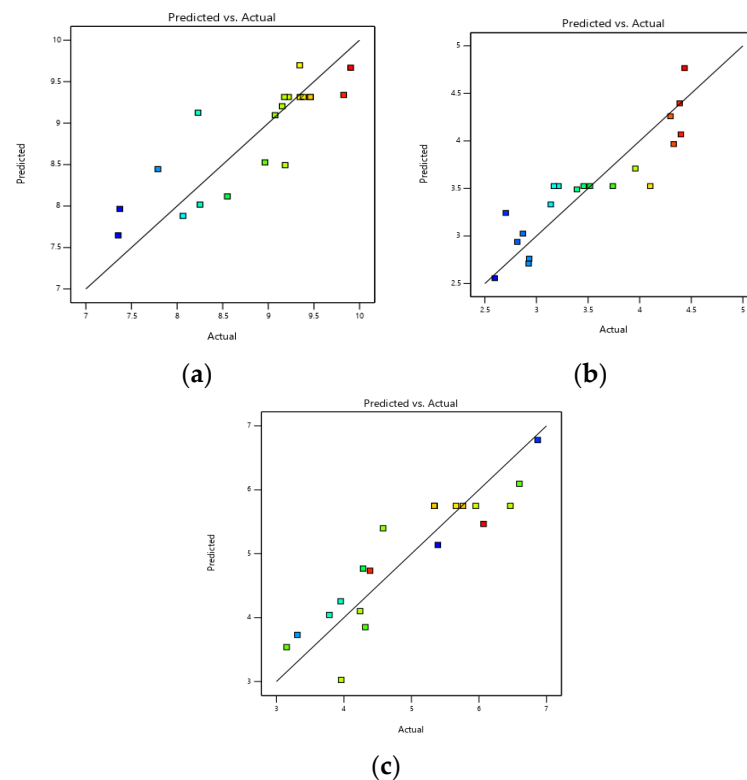
Table 2 showcases the results of the RSM studies obtained with Design Expert 13; the biomass was in the range of 5.03420 mg/L to 19.6730 mg/L. The COD removal efficiency was between 54.0890% and 98.0636%, and the range of power density generation was between 10.9574 mW/m<sup>2</sup> and 47.2064 mW/m<sup>2</sup>. The experimental data were fitted to four types of models: cubic polynomial, two-factorial interaction, linear, and quadratic. The statistical findings were found to be significant based on the sequential model sums of squares, as the obtained probability value (“prob > F”) was less than 0.05 (Table 3). The quadratic model was found to be the most suitable, as to the obtained *p* values of biomass, COD removal efficiency, and power density were less than 0.05, indicating their significance.

As shown in Table 3, the relationship between the three independent factors (biomass, COD removal efficiency, and power density generation) fit the model, as the *p*-values of all three responses for the model were less than 0.05, indicating their significance. Furthermore, lack-of-fit tests for all responses resulted in *p*-values of more than 0.05, indicating their insignificance.

The experimental data obtained in this study were also compared with the prediction data of the regression models. Figure 1 shows that the predicted values are generally centered on a straight line relative to the experimental data. This implies that there are relatively few deviations between the experimental values and the predicted values, supporting the quadratic model suggested by the ANOVA test. The normal plot residuals shown in Figure 2 also showcase the same pattern, in which the normal percentage probability points are centered near their respective straight lines. This indicates that the experimental data were normally distributed, consequently supporting the adequacy of the model [15].

**Table 2.** Result of biomass COD removal efficiency and power density generation obtained with CCD.

Std. Run	Code			Responses		
	A (CM)	B (%)	C (°C)	Y1: Biomass (mg/L)	Y2: COD Removal Efficiency (%)	Y3: Power Density (mW/m <sup>2</sup> )
1	0	0	−1	7.3050	54.0890	29.0647
2	+1	+1	+1	12.4500	98.0636	36.8210
3	0	+1	0	19.6730	87.3210	47.2064
4	0	0	+1	15.6650	60.6780	10.9574
5	+1	−1	−1	8.5540	65.0360	18.6340
6	0	−1	0	5.03420	54.3420	14.3210
7	0	0	0	11.0300	84.2100	41.7876
8	−1	+1	−1	17.3120	80.3410	43.5464
9	0	0	0	10.3270	88.0590	32.0320
10	0	0	0	11.9510	85.0320	35.4280
11	0	0	0	10.3420	87.3680	28.5430
12	+1	+1	−1	9.0340	82.3410	20.9806
13	−1	−1	+1	8.2300	84.3520	15.6780
14	0	0	0	12.3820	89.5111	33.2120
15	−1	+1	+1	19.2530	96.5629	19.2403
16	−1	−1	−1	5.8910	73.1260	18.3450
17	−1	0	0	9.8340	67.7263	15.6166
18	+1	0	0	9.8530	83.7556	17.9693
19	0	0	0	10.042	89.5111	28.4850
20	+1	−1	+1	7.9210	68.0720	9.9307

**Figure 1.** Comparison of predicted values and experimental values for (a) biomass, (b) COD removal efficiency, and (c) power density generation.

**Table 3.** ANOVA analyses of biomass, COD removal efficiency, and power density generation.

Response	Model Terms	Sum of Squares	df	Mean Square	F-Value	p-Value	
Biomass	Model	6.26	9	0.6955	4.71	0.0119	<b>significant</b>
	A: electrode distance	0.0303	1	0.0303	0.2051	0.6603	
	B: moisture content	5.89	1	5.89	39.91	<0.0001	<b>significant</b>
	C: temperature	0.2634	1	0.2634	1.78	0.0113	<b>significant</b>
	AB	0.0012	1	0.0012	0.0083	0.0292	<b>significant</b>
	AC	0.0006	1	0.0006	0.0041	0.0403	<b>significant</b>
	BC	0.0021	1	0.0021	0.0139	0.0185	<b>significant</b>
	A <sup>2</sup>	0.0233	1	0.0233	0.1578	0.6995	
	B <sup>2</sup>	0.0336	1	0.0336	0.2273	0.6437	
	C <sup>2</sup>	0.0043	1	0.0043	0.0291	0.8680	
	Lack of fit	0.8683	5	0.1737	1.43	0.0552	<b>not significant</b>
R <sup>2</sup>	0.8091						
COD Removal Efficiency	Model	7.98	9	0.8867	2.85	0.0392	<b>significant</b>
	A: electrode distance	0.0074	1	0.0074	0.0237	0.8808	
	B: moisture content	3.62	1	3.62	11.64	0.0066	<b>significant</b>
	C: temperature	0.7699	1	0.7699	2.47	0.1468	
	AB	0.3230	1	0.3230	1.04	0.0323	<b>significant</b>
	AC	0.0290	1	0.0290	0.0932	0.0166	<b>significant</b>
	BC	0.0952	1	0.0952	0.3060	0.0123	<b>significant</b>
	A <sup>2</sup>	0.0407	1	0.0407	0.1308	0.7251	
	B <sup>2</sup>	0.4200	1	0.4200	1.35	0.2723	
	C <sup>2</sup>	2.90	1	2.90	9.32	0.0122	<b>significant</b>
	Lack of fit	3.04	5	0.6080	42.19	0.0604	<b>not significant</b>
R <sup>2</sup>	0.8194						
Power Density Generation	Model	19.47	9	2.16	5.15	0.0086	<b>significant</b>
	A: electrode distance	0.0289	1	0.0289	0.0688	0.7984	
	B: moisture content	9.04	1	9.04	21.52	0.0009	<b>significant</b>
	C: temperature	2.39	1	2.39	5.69	0.0383	<b>significant</b>
	AB	0.0240	1	0.0240	0.0570	0.0161	<b>significant</b>
	AC	1.02	1	1.02	2.43	0.0101	<b>significant</b>
	BC	0.0730	1	0.0730	0.1736	0.0057	<b>significant</b>
	A <sup>2</sup>	4.44	1	4.44	10.56	0.0087	<b>significant</b>
	B <sup>2</sup>	0.2054	1	0.2054	0.4889	0.5004	
	C <sup>2</sup>	3.11	1	3.11	7.41	0.0215	<b>significant</b>
	Lack of fit	3.31	5	0.6613	3.69	0.0891	<b>not significant</b>
R <sup>2</sup>	0.8225						

*p*-values less than 0.0500 indicate that the model terms are significant; in this case, the model terms B, C, AB, AC, and BC are significant. For COD removal efficiency, model terms B, AB, AC, BC, and C<sup>2</sup> are significant. For power density, model terms B, C, AB, AC, BC, A<sup>2</sup>, and C<sup>2</sup> significant.

### Monitoring of Biomass, COD Removal Efficiency, and Power Density Generation

- Biomass

The highest biomass concentration observed in this study was 19.6730 mg/L, with ML-MFC parameters of 35 °C, 75% (*v/w*) moisture content, an electrode distance of 3 cm, and an incubation period of seven days (168 h), as designed with Design Expert 13 software.

The predicted significant interaction between the model terms for biomass was visualized by the previously acquired ANOVA results (Table 3) presented as response surface plots and contour plots.

Figure 3 displays the response surface plot and contour plot of the interaction between electrode distance and moisture content, Figure 4 presents the interaction between electrode distance and temperature, and Figure 5 displays the interaction of temperature with moisture content.



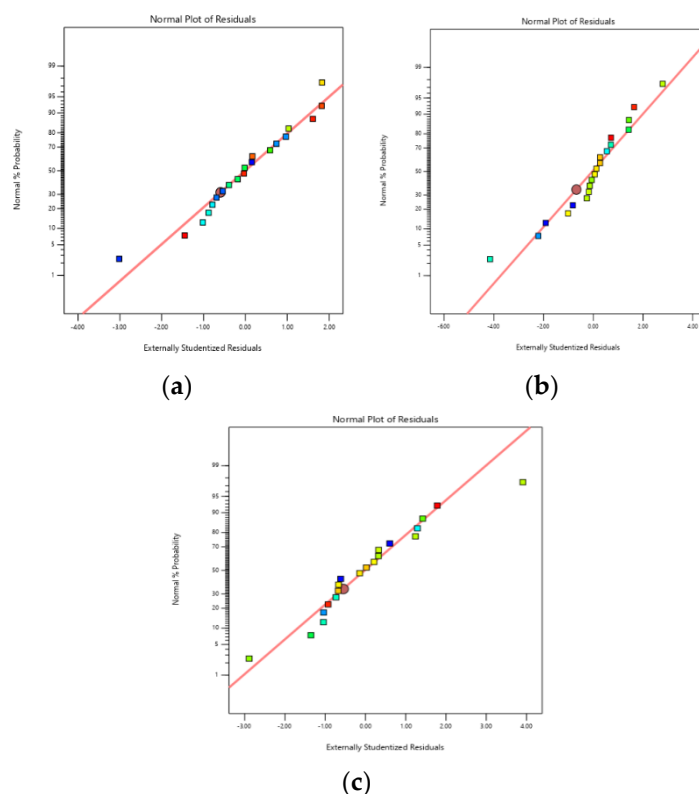


**Figure 2.** Normal plot of residuals for (a) biomass, (b) COD removal efficiency, and (c) power density generation.

Despite the more visualized aspect and a bigger overview figure provided by the response surface plot, the contour plot is relatively easier to interpret and understand with respect to the optimized values of the independent variables, for which the same level of responding variable can be achieved.

A higher concentration biomass is observed in Figure 3, wherein the moisture content level is approximately higher than 50% or, more precisely, higher than 60%, with an optimal electrode distance range of 3 cm. This is in line with the fact that a sufficient amount of moisture is required for the micro-organisms within the ML-MFC system to conduct hydrolysis reactions [15]. Additional water molecules are required by the microbes to break down the complex organic components. This breaking down of larger molecules into smaller molecules could ultimately aid in voltage generation in an ML-MFC system. This is due to the micro-organisms more easily consuming smaller compounds as opposed to the original larger compounds [15]. Due to the ease of digestion of the microbes, their metabolic reactions are further optimized. Consequently, the growth of biomass is now favorable, resulting in a higher biomass concentration obtained with increased moisture content. This phenomenon is also shown Figure 5; a higher biomass concentration was obtained at moisture content of more than 50% with an increase in temperature. This is also aligned with the acquired experimental data, as the highest biomass concentration was achieved with 60% moisture content (Table 2).

Figures 3 and 4 that the optimal range of electrode distance is 3 cm, as a higher concentration of biomass was attained under such conditions. An appropriate balance of electrode distance is required to achieve maximum performance of the ML-MFC system. This is because an excessive distance would result in undue resistance in the system [12], which would result in a decrease in voltage generation. This is due to a greater distance and time required for the protons to travel from anode to cathode in order to complete the circuit—also known as ohmic losses [12].

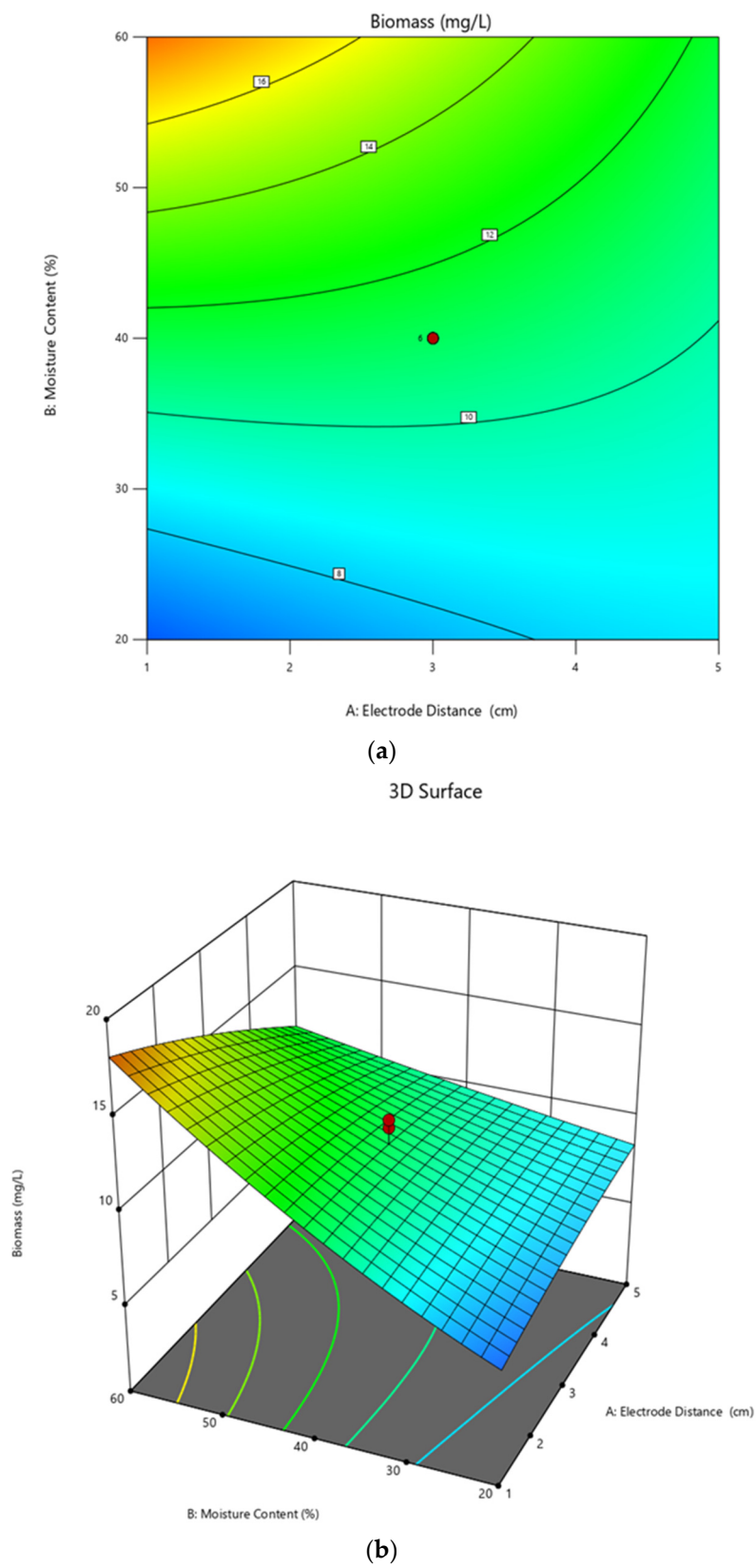


**Figure 3.** (a) Contour plot and (b) response surface plot of biomass as a function of moisture content relative to electrode distance.



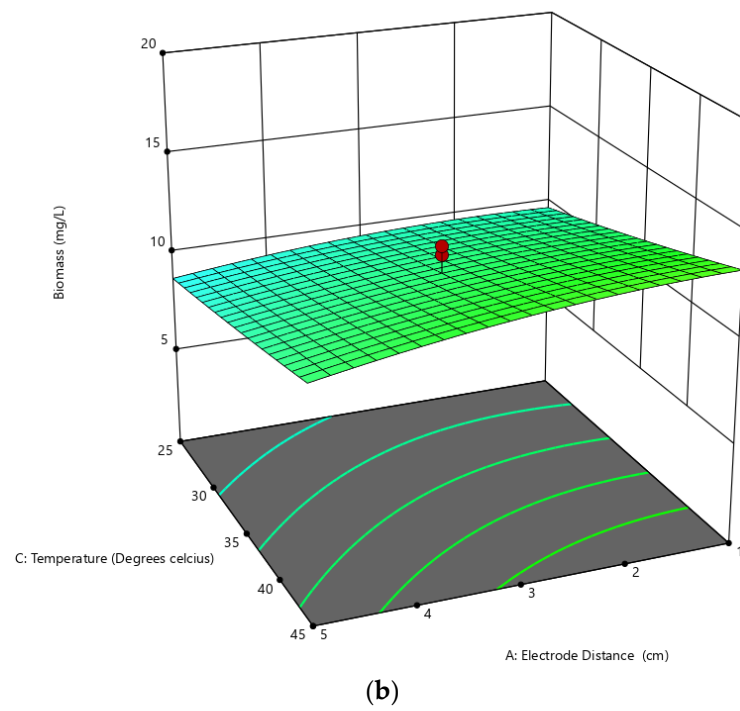
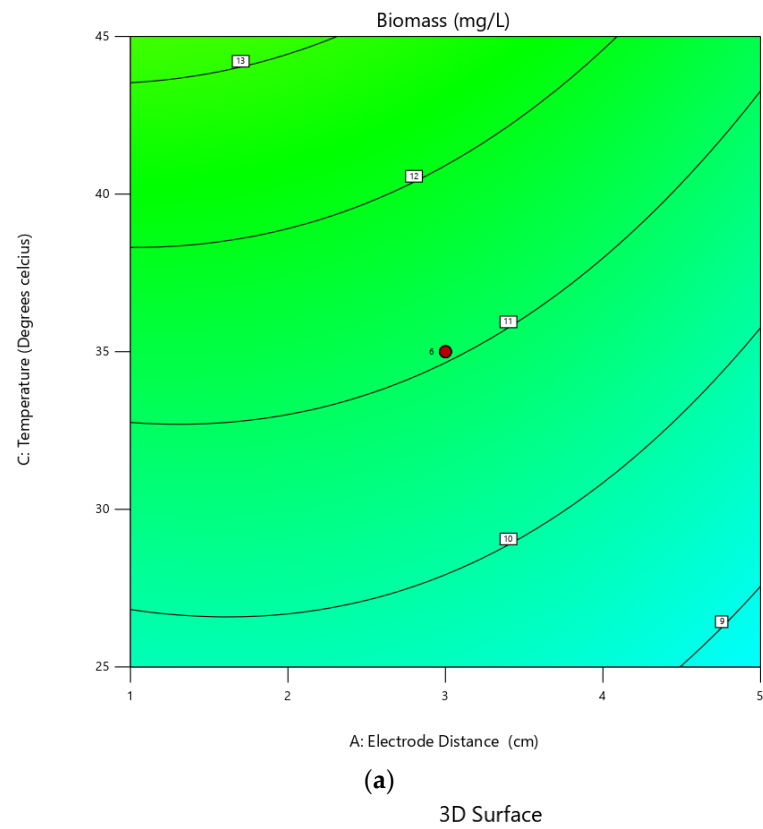


**Figure 4.** (a) Contour plot and (b) response surface plot of biomass as a function of temperature relative to electrode distance.

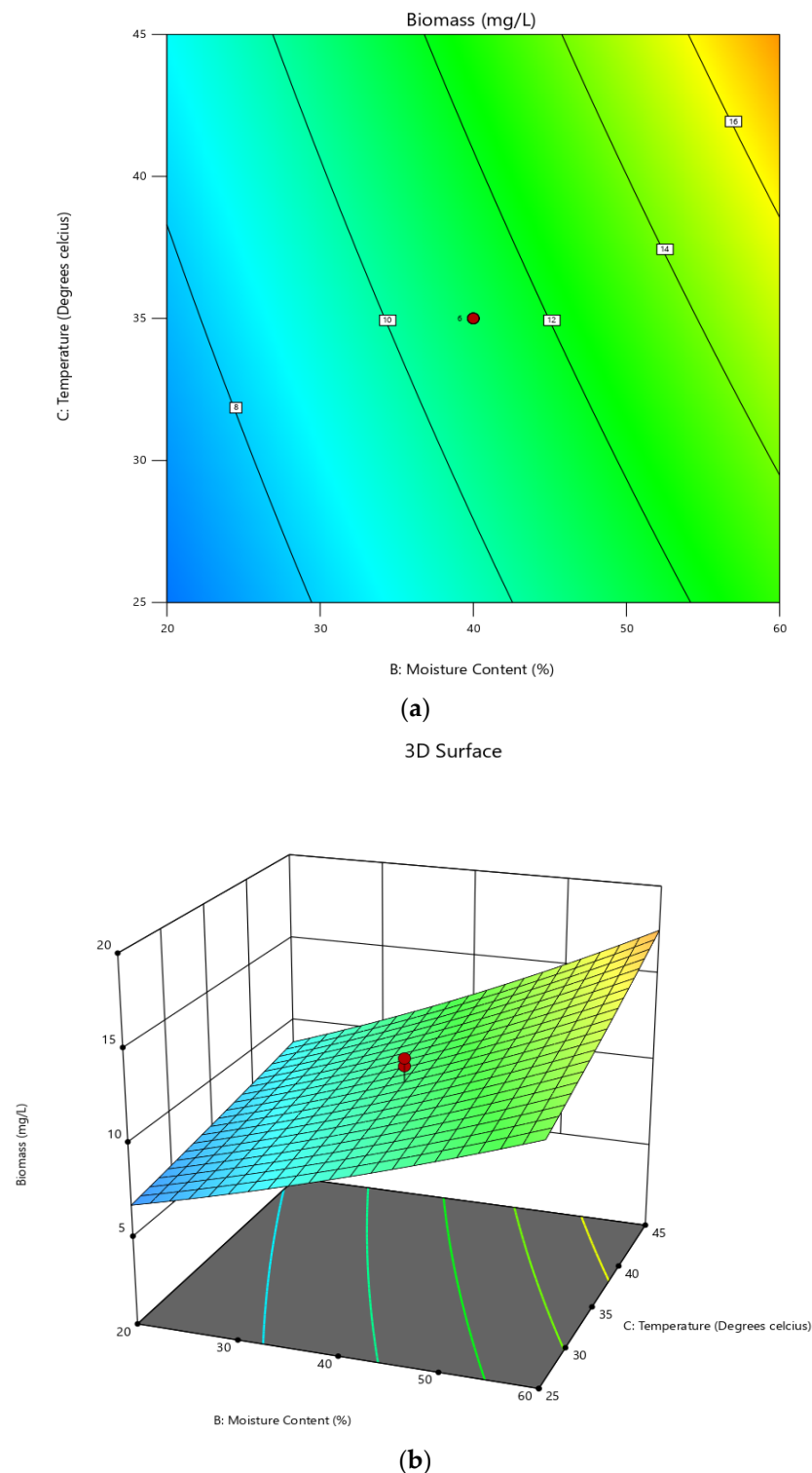


**Figure 5.** (a) Contour plot and (b) response surface plot of biomass as a function of temperature relative to moisture content.

Temperature levels also play a role in the performance of an ML-MFC system, whereby a temperature slightly higher than room temperature (27 °C) often promotes metabolic reactions of the cells within the MFC system. This could result in an improved growth rate of the cells within the system [15]. This is aligned with the obtained experimental data presented in Figures 4 and 5, with an increased biomass concentration at temperatures slightly below 35 °C. This occurred due to a higher rate of diffusion of organic matter present in the

substrate to the bacteria in the ML-MFC. However, an excessive temperature would lead to a decrease in the MFC's performance, as the temperature-sensitive components within the bacteria, such as nucleic acids and proteins, have the potential to be irreversibly damaged and would no longer function, as reported by Muaz (2019) [14].

- COD Removal Efficiency

In this research, the ML-MFC system obtained the highest COD removal efficiency at 98.0636% under the conditions of 35 °C, 75% (*v/w*) moisture content, an electrode distance of 3 cm, and an incubation period of seven days (168 h) as designed with Design Expert 13 software.

The contour plot and response surface plot of the interaction between moisture content and electrode distance are presented in Figure 6. Figures 7 and 8 present the contour and response surface plots of the interactions between temperature and electrodes, as well as between temperature and moisture content, respectively.

The phenomenon induced by an increase in moisture content previously mentioned with respect to biomass was also observed in relation to the COD removal efficiency, as shown in Figure 6; a higher percentage of COD removal efficiency was obtained with moisture content of more than 50% (closer to 60%). This condition was also paired with an approximate optimal electrode distance of 3 cm. This phenomenon is also shown in Figure 8; the optimal range of moisture content is also proximately higher than 50%, with an optimal range of temperature of roughly 35 °C to 45 °C. The additional moisture content boosts the COD removal efficiency, as the increased amount of complex matter in the substrate can now be broken down into simpler molecules. This is a result of the increased ease with which microbes can conduct hydrolysis reactions within the ML-MFC system [14], resulting in higher COD removal efficiency values.

The same phenomenon with respect to the effect of electrode distance is shown in Figures 7 and 8; a higher percentage of COD removal efficiency was achieved at approximately 3 cm with paired optimal conditions of moisture content higher than 50% and temperature ranging from 35 °C to 40 °C, respectively.

Temperatures of approximately 35 °C were observed to be optimal, as shown in Figures 7 and 8; a higher percentage of COD removal efficiency is shown in both figures. This occurred as a consequence of the enhanced microbial metabolic reactions that took place, as mentioned with respect to biomass, due to the increase in temperature, resulting in improved substrate consumption by the bacteria in the MFC. In a domino effect, an increased amount of complex matter was broken down into smaller matter, resulting in increased COD removal efficiency.

- Power Density Generation

The greatest power density generation obtained by the ML-MFC system in this study was 47.2064 mW/m<sup>2</sup>, operating at 35 °C, 75% (*v/w*) moisture content, and an electrode distance of 3 cm, with an incubation period of seven days (168 h), as designed with Design Expert 13 software.

The contour plot and response surface plot of the interactions between moisture content and electrode distance, temperature and electrode distance, and temperature and moisture content are shown in Figures 9–11, respectively.

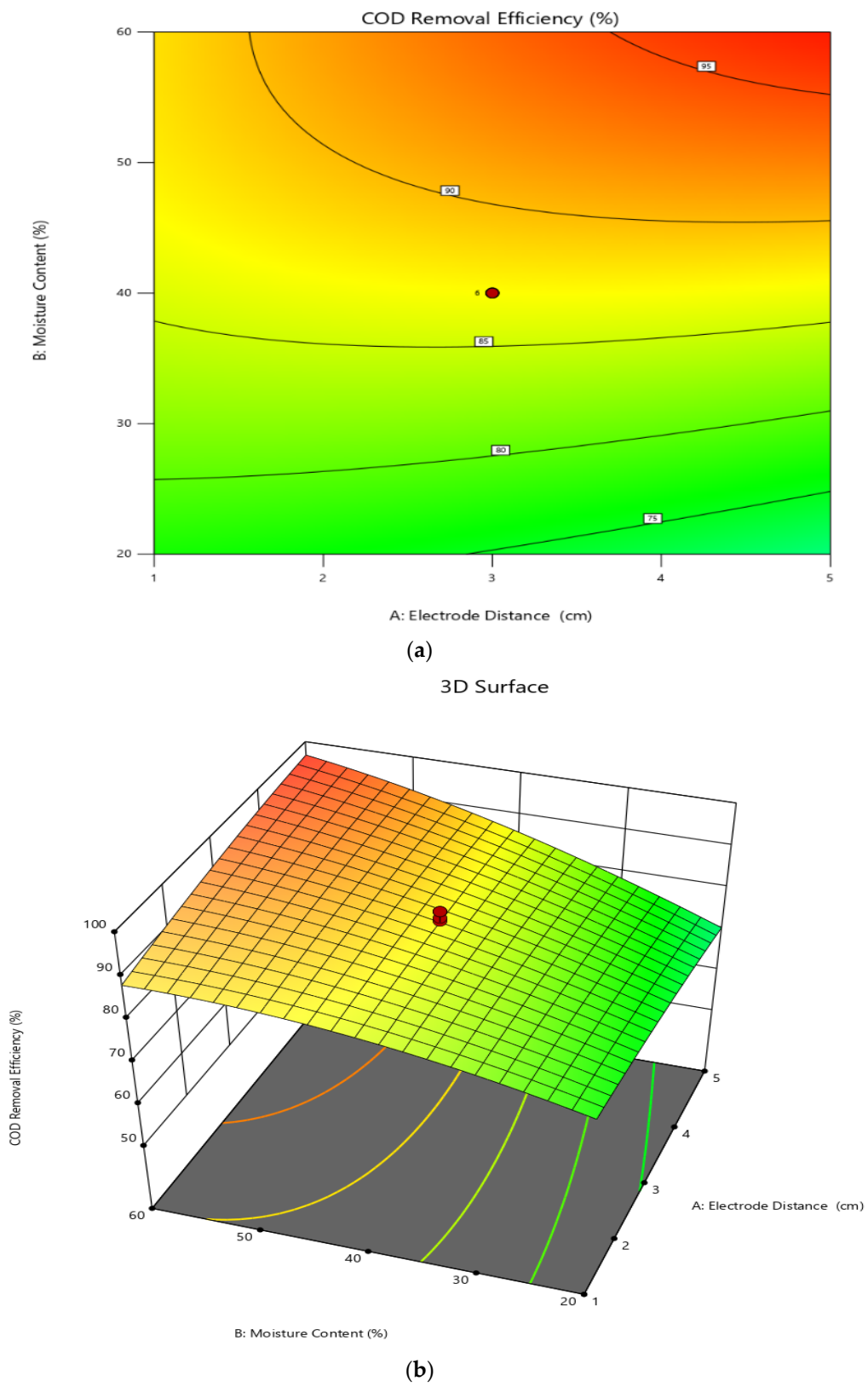


**Figure 6.** (a) Contour plot and (b) response surface plot of biomass as a function of moisture content relative to electrode distance.

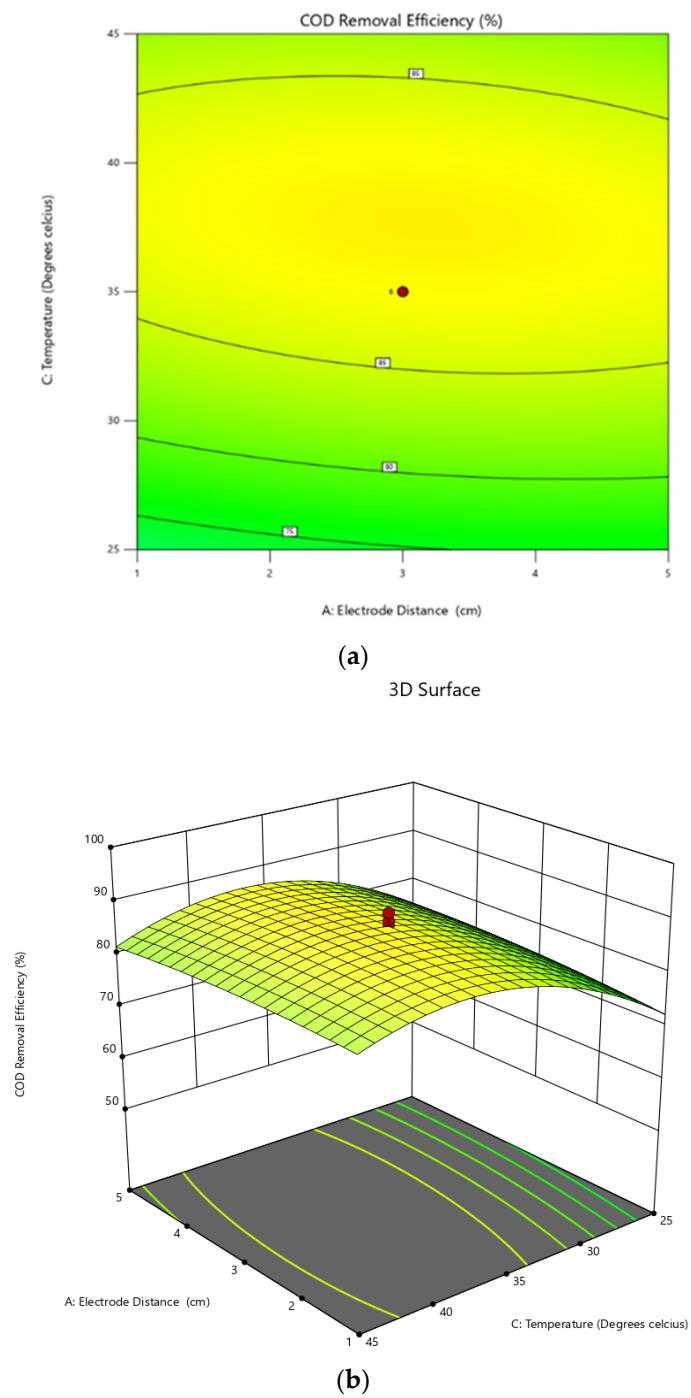
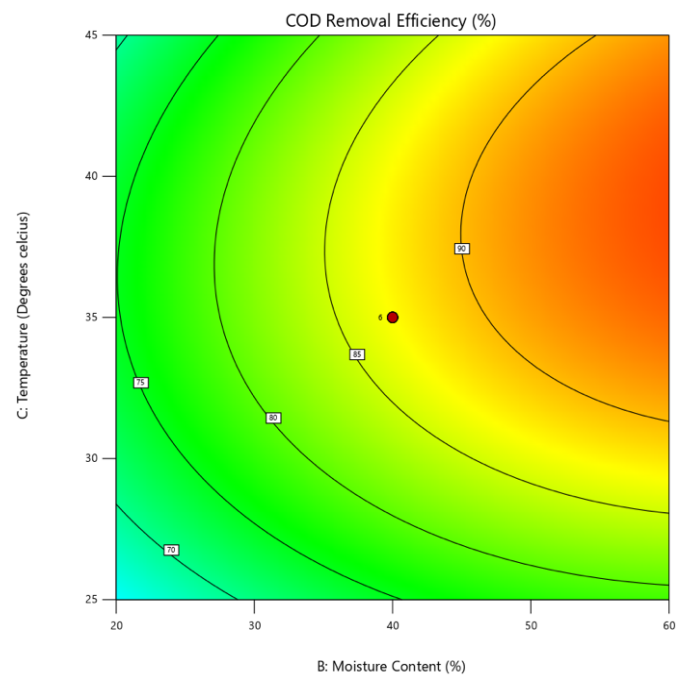
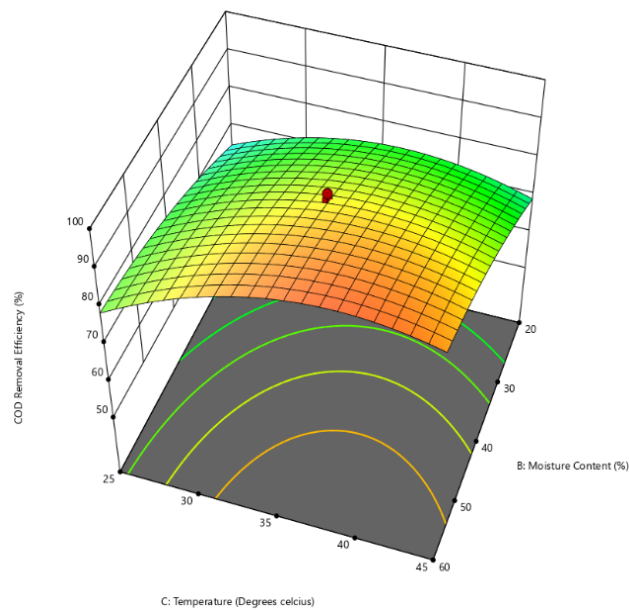


**Figure 7.** (a) Contour plot and (b) response surface plot of COD removal efficiency as a function of temperature relative to electrode distance.



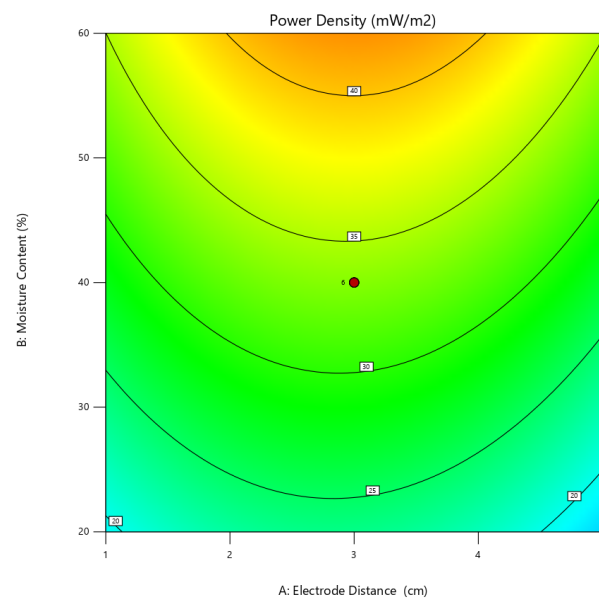
(a)  
3D Surface



(b)

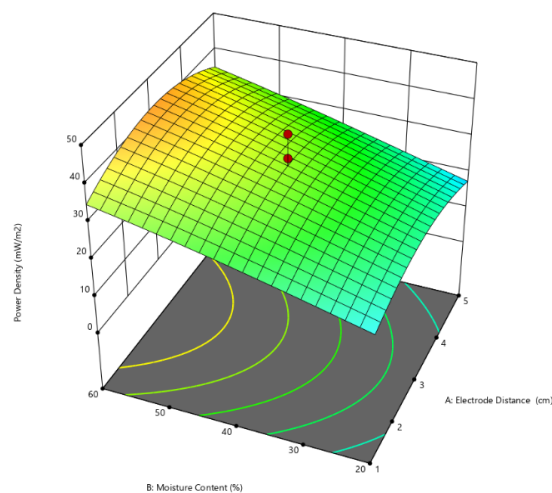
**Figure 8.** (a) Contour plot and (b) response surface plot of COD removal efficiency as a function of temperature relative to moisture content.





(a)

3D Surface

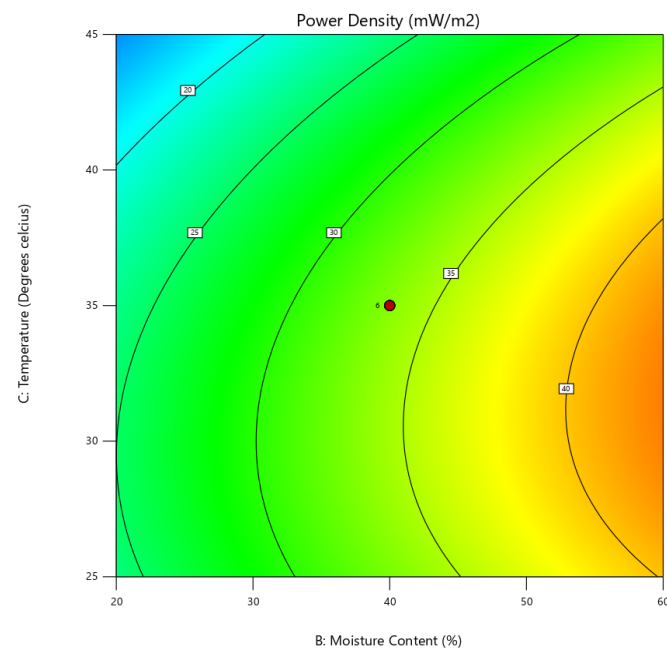


(b)

**Figure 9.** (a) Contour plot and (b) response surface plot of power density generation as a function of moisture content relative to electrode distance.

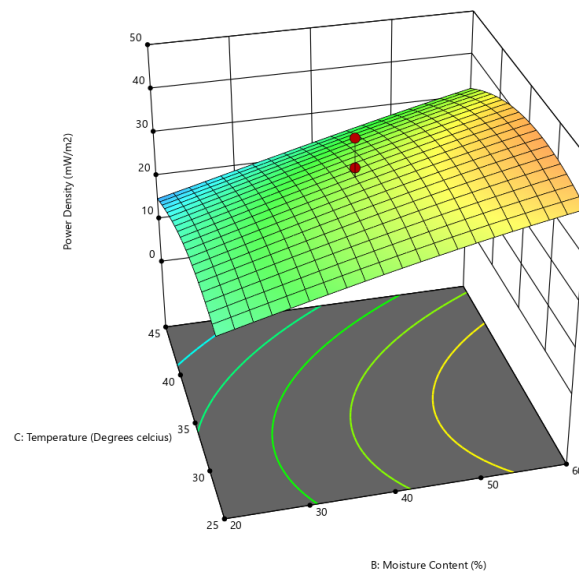
Similar to the impact on biomass concentration and percentage of COD removal efficiency, the ML-MFC system with a higher level of moisture content also generated a higher power density with a moisture content of more than 50%, as shown in Figures 9 and 10, with an optimal temperature range of approximately 35 °C and an electrode distance of 3 cm.

As observed with respect to biomass and COD removal, higher power density generation was also observed, as shown in Figures 9 and 11, with an electrode distance of 3 cm, similar to the high biomass concentration percentage of COD removal efficiency. This is due to an appropriate distance between the anode electrode and the cathode electrode, avoiding the occurrence of ohmic losses in the system [12].



(a)

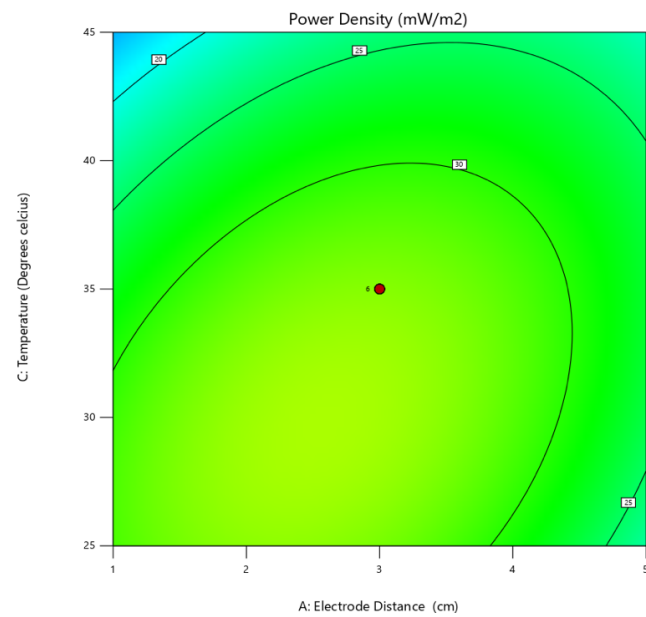
3D Surface



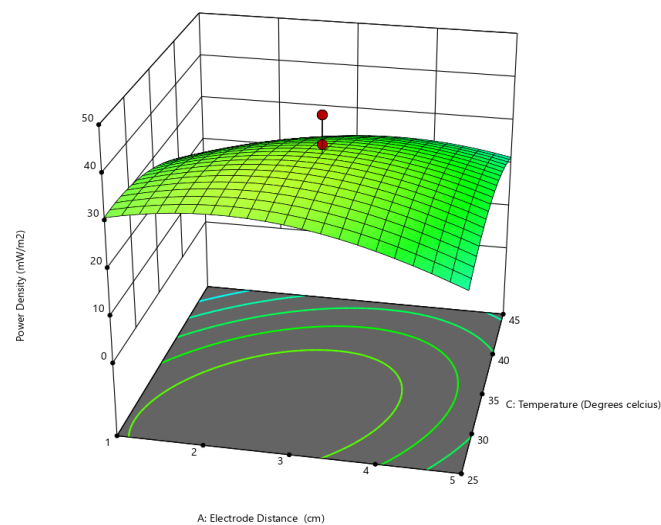
(b)

**Figure 10.** (a) Contour plot and (b) response surface plot of power density generation as a function of temperature relative to moisture content.

A higher power density generation was attained in the temperature range of approximately 27 °C to 37 °C, as shown in Figures 10 and 11, accompanied by an optimal electrode distance of about 3 cm and a moisture content of more than 50%. This is due to the ease with which bacteria can carry out their metabolic reactions, leading to increased substrate degradation within the ML-MFC system. Therefore, transfer of electrons from bacteria to the anode electrode increased, enabling a faster reaction and leading to increased power density generation.



(a)  
3D Surface



(b)

**Figure 11.** (a) Contour plot and (b) response surface plot of power density generation as a function of temperature relative to electrode distance.

#### Optimum Range of Parameters and Validation of Models

The optimum conditions required for the ML-MFC system in this study to generate the greatest biomass, COD removal efficiency, and power density generation are presented in Table 4. Optimization of the experimental study is essential to establish the optimal conditions of the ML-MFC system. The conditions showcased in Table 4 were suggested by DesignExpert13 software based on statistical analyses.

**Table 4.** Optimal conditions suggested by Design Expert 13 software.

Parameter	Unit	Value
Electrode distance	cm	5.00
Moisture content	%	60.00
Temperature	°C	34.58
Response 1:biomass	mg/L	17.16
Response 2: COD removal efficiency	%	75
Response 3:power density generation	mW/m <sup>2</sup>	36.25
Desirability		0.899

In validating the optimal conditions suggested by Design Expert 13 software represented in Table 5, an additional five runs were conducted in order to evaluate the accuracy of these conditions. The results obtained from the additional runs are presented in Table 5; both mean and standard deviation values for the experimental runs were calculated. A confidence level of approximately 95% was determined based on comparison of the experimental data with the predicted data.

**Table 5.** Comparison between experimental data and predicted data for the optimal conditions suggested by Design Expert 13 software.

Run	Response 1: Biomass (mg/L)			Response 2: COD Removal Efficiency (%)			Response 3: Power Density Generation (mW/m <sup>2</sup> )		
	Exp.	Pred.	$\epsilon$	Exp.	Pred.	$\epsilon$	Exp.	Pred.	$\epsilon$
1	16.61	17.16	−0.55	73.47	75	−1.53	37.81	36.25	1.85
2	16.58	17.16	0.42	76.85	75	1.85	38.10	36.25	−1.16
3	17.77	17.16	0.61	78.31	75	3.31	35.09	36.25	0.33
4	16.98	17.16	−0.18	71.47	75	−3.53	36.58	36.25	1.41
5	17.38	17.16	0.22	77.63	75	2.63	37.66	36.25	0.798
Mean	17.064	17.16	0.104	75.546	75	0.546	37.048	36.25	0.6456
SD		0.4684			2.9413			1.2363	
95% CI		16.30–18.02			71.25–78.75			34.44–38.06	

Note: Exp. = experimental data, Pred. = predicted data,  $\epsilon$  = error, SD = standard deviation, 95% range within 95% confidence level.

According to our obtained results, we found that operating conditions of an ML-MFC system can be optimized through the utilization of RSM via CCD for biomass, COD removal efficiency, and power density generation. As shown in Table 5, the results of the validation tests did deviate substantially from the predicted values proposed by RSM. This is because the obtained experimental values for biomass, COD removal efficiency, and power density generation are all still within the respective range of 95% confidence level (16.30–18.02 mg/L, 71.25–78.75%, and 34.44–38.06 mW/m<sup>2</sup>, respectively). Therefore, based on the validation test, we can conclude that the operating parameters of and ML-MFC can be optimized via RSM (CCD).

### 2.3. ML-MFC Performance

#### 2.3.1. Polarization Curve

The ML-MFC conditions proposed by RSM (Table 4) were evaluated in terms of performance via polarization curve technique (Figure 12), whereby current and power densities were calculated using the following equation: ( $P = \frac{IV}{A}$ ). As shown in Figure 12 and Table 2, the studied ML-MFC system achieved the highest power density at 47.2064 mWm<sup>−2</sup>. This obtained power density value is approximately equal to the power density (blue line color in obtained in other studies in which soil or waste were also employed [14] (41.3 mWm<sup>−2</sup>) and as reported by Logan and Regan [16] at 43.1 mWm<sup>−2</sup>. This suggest that the substrate utilized in this study (dewatered sludge supplemented with chicken manure) has the

potential to be employed as a substrate for ML-MFC systems, as we obtained a higher power density than those reported above.

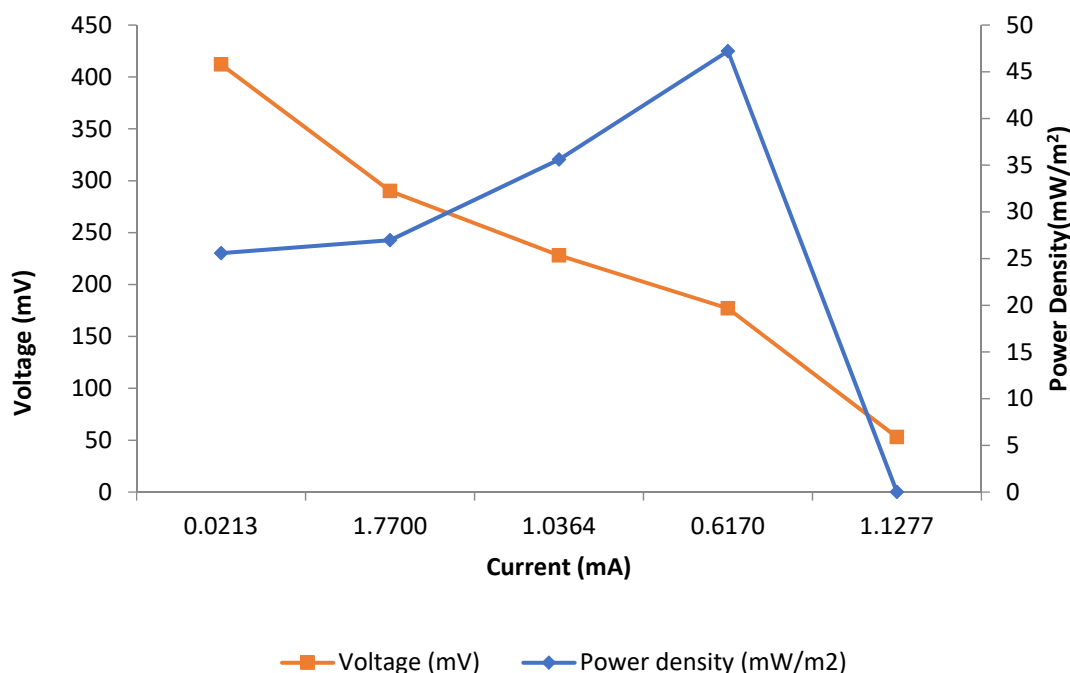


**Figure 12.** Polarization curve of ML-MFC.

According to the polarization curve, the ML-MFC system can undergo three phases of losses, namely activation losses, ohmic losses, and concentration losses (line orange color in Figure 12) [12]. This was interpreted as such in the polarization curve due to its general trend. The system underwent activation losses when the ML-MFC voltage had rapidly dropped from 412 mV to 290 mV. Activation losses are losses that take place within the ML-MFC system as a result of energy loss caused by redox reactions that required energy to accomplish reactions [12]. This occurs when electrons are transferred to or from the substance of its designated electrodes (anode and cathode). The substance or compound can exist on the surfaces of the microbes or electrodes. By reducing such losses, the operating temperature of the ML-MFC system can be increased to facilitate the energy required for electron transfer [12]. This was observed in the case of the ML-MFC tested in the present study; systems operating at higher temperatures performed better than those operating temperatures of less than 35 °C, as shown in Table 2 and Figure 8. However, an excessive temperature could also result in voltage losses, as there are many temperature-sensitive components in the substrate, such as proteins. Such components are prone to heat damage if they are exposed to high temperatures, consequently hindering bacterial performance [17].

The ML-MFC system also experienced ohmic losses from 290 mV to 177 mV, with a less rapid voltage drop than that associated with activation losses. Ohmic losses occur as a result of interference with electron propagation toward the final acceptor (oxygen) from cathode to anode. Hence, the greater the required propagation of electrons, the greater the risk of ohmic losses. Accordingly, reducing the electrode distance is an option to reduce ohmic losses in the system, as electrons no longer have to travel as far [12]. However, the electrode distance should also not be too short, which could lead to crossing over of oxygen molecules from cathode (location of the final electron acceptor) to anode. This would result in reduced voltage generation, as there would be fewer electron acceptors at the cathode to complete the proton transfer pathway for the generation of energy [13].

The ML-MFC was also interpreted to have experienced concentration losses when its voltage dropped from 177 mV to 53 mV (Figure 12), which is less of a voltage drop compared to the previous drop. Concentration losses in an MFC occur when the rate of

mass transport of compounds between the electrodes are interfered with by the generation of current. This can occur as a result of high ratios between the oxidized compounds and reduced compounds at the anode surface within the system [12]. This phenomenon was caused by organic compounds in the substrate being oxidized at a faster rate at the anode than the rate at which they were transported to the surface [12]. The polarization curve can be interpreted to have undergone the three mentioned phases of losses, as its general trend of an initially rapid voltage followed by a slower voltage drop and, finally, an even lower voltage inevitably took place, as mentioned above. In further maximizing the performance of an MFC system, each of the losses should ideally be reduced in the future.

### 2.3.2. Comparison between Biomass Growth in Shake Flask and MFC Systems

The kinetic growth profile (doubling time ( $T_d$ ) and specific growth rate ( $\mu$ )) of BS was calculated with equations presented in Appendices A–C. Doubling time is the period of time that is required for the population size of bacteria to double. Due to the more active reactions, cell mass and cell number density increase exponentially with time. Specific growth rate is known as the rate at which a cell population's biomass increases per unit of biomass concentration.

The acquired specific growth rate and doubling time of BS were  $0.0533 \text{ h}^{-1}$  and 12.9972 h, respectively (Table 6). The highest specific growth rate and the earlier doubling time provided the cells with full potential to develop maximum biomass in a shorter period of time. The values of  $\mu$  and  $T_d$  in the ML-MFC were calculated as  $0.0177 \text{ h}^{-1}$  and 39.08 h, respectively. There is a slight difference in the growth of BS in a shake flask as opposed to an ML-MFC system.

**Table 6.** Kinetics growth profile of BS growth using chicken manure supplemented with sludge in shake flask and in ML-MFC systems.

Condition	Doubling Time, $T_d$ (h)	Specific Growth Rate, $\mu$ ( $\text{h}^{-1}$ )
Shake flask	12.9972	0.0533
ML-MFC	39.08	0.0177

According to Table 6, the  $\mu$  and  $T_d$  values for dewatered sludge supplemented with chicken manure in the ML-MFC system were  $0.0177 \text{ h}^{-1}$  and 39.08 h, respectively, whereas for the growth of BS in the shake flask system, the values for  $\mu$  and  $T_d$  were  $0.0533 \text{ h}^{-1}$  and 12.9972 h, respectively. The higher  $\mu$  value and the earlier  $T_d$  period indicates that the BS has the ability to generate maximum biomass productivity in a shorter period of time. BS performed better in the shake flask system due to the external agitation provided by the incubator shaker. This allowed for improved distribution of nutrients in the culture, better facilitated the diffusion of nutrients into the cells. Consequently, the cells were able to grow at a faster specific growth rate and with a shorter doubling time with degradation by BS-generated electrons, improving the power generation of ML-MFC. Although there was a difference in the values of  $\mu$  and  $T_d$  between these two substrate conditions, the growth profile of both systems showed the same trend.

### 2.3.3. Biomass and Power Density Generation

The general trend of biomass concentration and power density generation of the best-performing ML-MFC system obtained by the experimental data (Table 2) at 75% moisture content, 3 cm of electrode distance, and  $35 \text{ }^\circ\text{C}$  is shown in Figure 13. In the early stages of the incubation period (0 h until 12 h), the power density generation remained zero, despite the presence of microbial growth. This is due to the activation losses that took place within the system due to the bacterial requirement of energy to carrying out metabolic reactions [12]. This led to a utilization of energy for such activities, as opposed to power generation, resulting in a lack of power generation during the early incubation period.



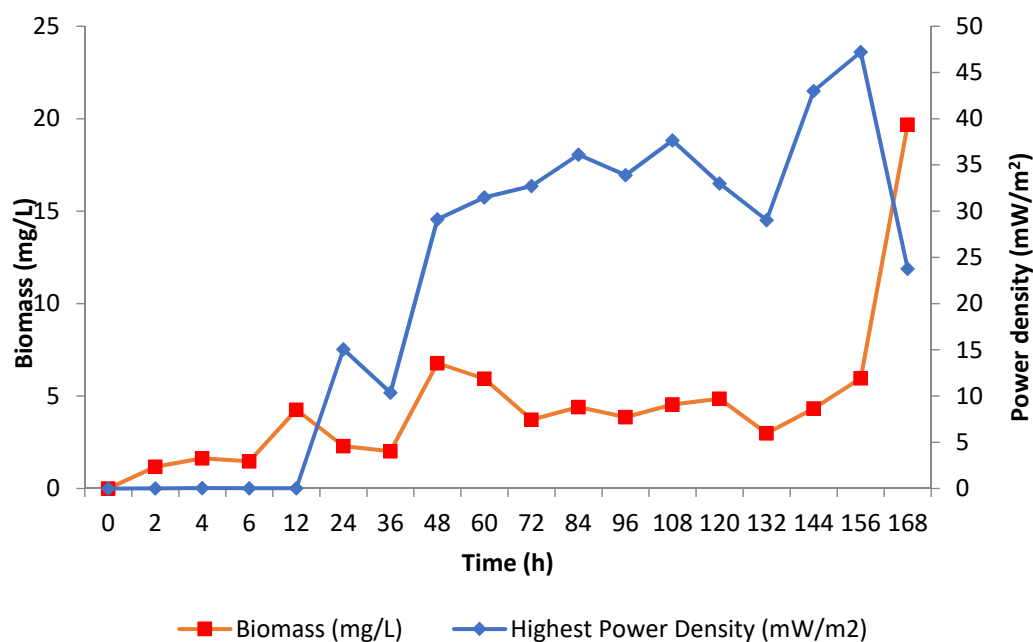


**Figure 13.** Profile of biomass and power density generation during the incubation period.

After 12 h, the ML-MFC experienced fluctuations in power generation, as well as in its biomass growth, until it reached peak power generation in the 156th hour at 47.2064 mW/m<sup>2</sup>. In this phase, the ML-MFC system appeared to operate at maximum efficiency. There was a sharp increase in power generation following the lower power generation in the beginning of the incubation period from the 36th hour to the 48th hour from 10.3620 mW/m<sup>2</sup> to 29.1128 mW/m<sup>2</sup>. This is due to the ability of the bacteria to degrade a greater number of complex molecules, which, in turn, would lead to increased power generation compared to previous hours. This is because the bacteria now has secreted a sufficient number enzymes to facilitate the degradation of the complex molecules into simpler compounds, which could then be utilized by the microbes to carry out metabolic activities [14], resulting in increased generation of power in a shorter period of time.

After the 48th hour, minor fluctuations in power generation took place; however, there was a general trend of increasing of power generation throughout the incubation period, as well as a sharp decrease in power generation (from 47.2064 mWm<sup>-2</sup> to 23.7650 mWm<sup>-2</sup>) and a sharp increase in biomass from 1.965 mg/L to 19.673 mg/L. This is due to the increased bacteria population utilizing the energy present in the ML-MFC system for its own metabolic reactions, resulting in a sharp decrease in power generation [12].

### 3. Methodology

#### 3.1. Sample Collection

The dewatered sludge sample was collected at Indah Water KonsortiumMakMandin, Butterworth, Malaysia. The chicken manure sample was collected at Permatang Berangan Tasek Gelugor, Penang. Both samples were kept at 4 °C for storage purposes and were later thawed to room temperature (27 °C) prior to use according to the method described by Muaz(2019) [14].

#### 3.2. ML-MFC Construction

The ML-MFC device was comprised of cylindrical PVC reactors with a diameter of 6.5 cm and a height of 10 cm. Graphite anodes and cathodes were placed at the bottom and top of the reactor, respectively, with the substrate (dewatered sludge supplemented with chicken manure) placed in between at various depths ranging from one cm to six cm. The substrate, which acted as the pseudo-membrane, was kept moist with 10% inoculum, as well as the addition of deionized water (Figure 14). The graphite electrodes were 3.25 cm in

radius and 0.65 cm in thickness, with a surface area of 33.18 cm<sup>2</sup> (0.0033 m<sup>2</sup>). The device was also capped with a lid with two holes for the electrode probes to measure electricity generation of the ML-MFC using a digital multimeter (UT33D, UNI-T, Hong Kong).

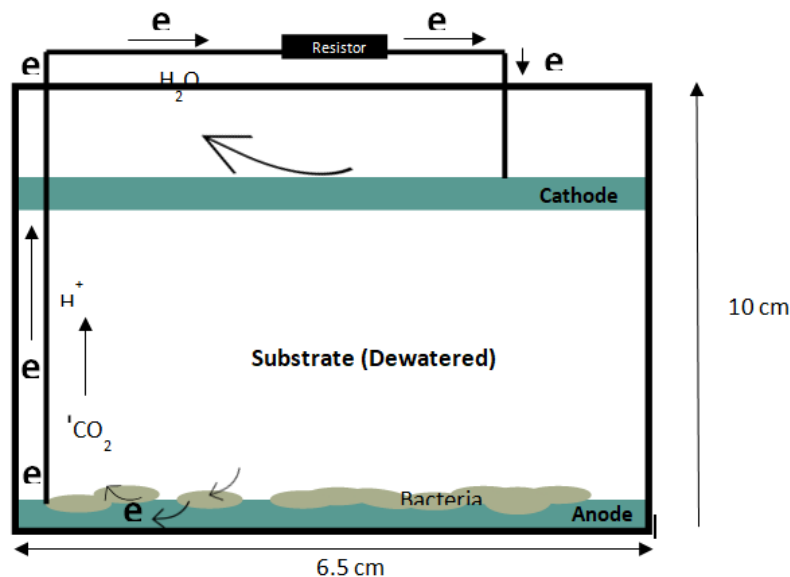


**Figure 14.** Illustration of membrane-less air cathode.

### 3.3. Operation of ML-MFC

In this study, the effects of electrode distance, moisture content, and temperature on voltage generation, as well as COD removal within the system, were studied. In evaluating the effect of electrode distance, the substrate depth in the ML-MFC was varied. The effect of moisture content on the ML-MFC system was observed by varying the substrate's moisture from 10% to 75% (vol/wt.) with sterile deionized water. To determine the effect of temperature on the ML-MFC's performance, the system temperature was varied from 25 °C to 52 °C. For all the studies above, the ML-MFC devices were incubated for seven days, and voltage and COD values were recorded every twelve hours using a multimeter and UV-Vis DR 2800 following method COD 8000.

### 3.4. Statistical Experimental Design

Optimization of Electricity Generation by Response Surface Methodology via Central Composite Design (CCD)

A statistical tool, response surface methodology (RSM) via CCD, was utilized in this project to further study the relationship of three [3] independent variables (distance between electrodes (A), moisture content (B), and temperature (C)) with three responses (biomass (Y1), COD removal efficiency (Y2), and power density (Y3) (Tables 7 and 8).

**Table 7.** Variable levels determined via RSM-CCD.

Factor (Symbol)	Variable	Coded Variable Level		
		Low	Centre	High
		−1	0	+1
A	Electrode distance (cm)	1	3	5
B	Moisture content (%)	20	40	60
C	Temperature (°C)	25	35	45

**Table 8.** Proposed conditions of electrode distance (cm), moisture content (%), and power density ( $\text{mW}/\text{m}^2$ ) for the ML-MFC systems determined by CCD.

Std. Run	Code		
	Electrode Distance (A)	Moisture Content (B)	Temperature (C)
	cm	%	$^{\circ}\text{C}$
1	3	40	18.1821
2	5	60	45
3	3	73.6359	35
4	3	40	51.8179
5	5	20	25
6	3	6.36414	35
7	3	40	35
8	1	60	25
9	3	40	35
10	3	40	35
11	3	40	35
12	5	60	25
13	1	20	45
14	3	40	35
15	1	60	45
16	1	20	25
17	0	40	35
18	6	40	35
19	3	40	35
20	5	20	45

- Effect of Electrode Distance Variation

In studying the effect of electrode distance variation, the distance between the anode and cathode electrodes was manually varied by the addition of substrate (dewatered sludge and chicken manure) in between the electrodes until the desired distance was achieved. The substrate at the bottom remained uninterrupted.

Voltage and power density generation, biomass detection, and COD removal efficiency detection (described in Sections 3.5.4–3.5.6) were conducted every two hours until the sixth hour, every six hours until the twelfth hour, and every twelve hours up the 168th hour (seven days) of the incubation period.

- Effect of Moisture Content Variation

In studying the effect of moisture content variation, the moisture content of the system was manually varied from 10% to 75% by the addition of deionized water to the substrate mixture. Voltage generation, power density generation, biomass detection, and COD removal efficiency detection were carried out as in section on the Effect of Electrode Distance Variation.

- Effect of Temperature Variation

In evaluating the effect of temperature variation in this study, the temperature was varied from 18  $^{\circ}\text{C}$  to 52  $^{\circ}\text{C}$  through the utilization of incubators capable of varying temperature. For conditions requiring a temperature lower than 30  $^{\circ}\text{C}$ , a laboratory fridge was utilized for temperatures between 18  $^{\circ}\text{C}$  and 25  $^{\circ}\text{C}$ . Voltage generation, power density generation, biomass detection, and COD removal efficiency detection were monitored as described in the section on the Effect of Electrode Distance Variation.

### 3.5. Analytical Methods

#### 3.5.1. Elemental Analysis

The carbon (C), hydrogen (H), and nitrogen (N) contents present in the dewatered sludge and chicken manure samples were detected using an elemental analyzer (PerkinElmer

2400 series II). The samples underwent preparation prior to elemental analysis, as the analyzer necessitates a small amount of sample to be in a solid form. Sample preparation involved oven drying the dewatered sludge and chicken manure for 24 h at 60 °C and for 6 h at 60 °C, respectively. The dried samples were then used for analysis. During the analysis, the samples were subjected to purified helium, compressed air, and oxygen being purged into the analyzer at 20, 60, and 15 psi, respectively. Combustion and reduction furnaces were operated at 9758 °C and 5008 °C, respectively.

### 3.5.2. Atomic Absorption Spectrophotometry (AAS) Analysis

Trace elements in the samples, such as iron (Fe), manganese (Mn), magnesium (Mg), cadmium (Cd), and zinc (Zn), were detected through atomic absorption spectrometry (AAS) (SHIMADZU, model ASC-700). The samples underwent a digestion process (sample preparation) prior to AAS analysis using concentrated acids to acquire absolute purity samples. A total mass of one g sample was weighed, and total volumes of ten mL and one mL of concentrated HNO<sub>3</sub> and concentrated H<sub>2</sub>O<sub>2</sub>, respectively, was added to the sample in a digestion vessel under a fume hood. The sample then underwent a digestion process in a microwave digester for approximately one hour before being left to cool to room temperature (27 °C). The digested sample was then transferred into a 50 mL volumetric flask and topped up with deionized water, affording a standard sample stock culture. The standard sample stock culture was then utilized for AAS analysis after filtration of sample particulates using filter paper (Whatman No.42, Maidstone, UK). Standards for elements that were utilized for the analysis were 1000 ppm.

### 3.5.3. Inductively Coupled Plasma Optical Emission (ICP–OES) Analysis

Micronutrients present in the samples, such as phosphorus (P) and potassium (K), were detected using ICP-OES. The sample underwent a digestion process (sample preparation) prior to analysis using concentrated acids to obtain pure samples. A total mass of one gram sample was weighed, and total volumes of ten mL and one mL of concentrated HNO<sub>3</sub> and concentrated H<sub>2</sub>O<sub>2</sub>, respectively, were added to the sample in a digestion vessel under a fume hood. The sample then underwent a digestion process in a microwave digester for approximately one hour before being left to cool to room temperature (27 °C). The digested sample was then transferred to a 50 mL volumetric flask and topped up with deionized water, affording a standard sample stock culture. The standard sample stock culture was then utilized for the ICP-OES analysis following filtration of sample particulates using filter paper (Whatman No.42). Standards for elements that were utilized for the analysis were 1000 ppm.

### 3.5.4. Chemical Oxygen Demand (COD) Analysis

COD analysis was performed to determine substrate degradation efficiency. A total mass of 1 gram of sample was diluted with a volume of 9 mL of deionized water in a 15 mL falcon tube. Syringe filters (MF-Millipore Millex GS syringe filter with a pore size 0.22 µm) were used to filter the sample. A total volume of two mL of filtrate was added to COD vials containing a premixed chemical solution (K<sub>2</sub>Cr<sub>2</sub>O<sub>7</sub>, AgNO<sub>3</sub>, and H<sub>2</sub>SO<sub>4</sub>). The filtrate-containing COD vials were then digested (Lovibond Thermoreactor, RD125) at 150 °C for two hours and then cooled to room temperature (27 °C). The COD values of the digested samples were then read using UV-Vis DR 2800 following method COD 8000.

### 3.5.5. Power Generation Using the Polarization Curve Technique

A polarization curve technique was utilized in this study to determine the electricity generation and performance of the ML-MFC. The cell voltage measurements of the ML-MFC were read and recorded at open circuit voltage and at different external resistances (47, 100, 220, 470, and 1000 Ω). The output of electrical power was then determined using Ohm's law ( $R = \frac{V}{I}$ ) and  $P = VI$ , with which the power density generations were acquired by dividing the power values by the ML-MFC surface area ( $P = \frac{IV}{A}$ ). Based on these acquired values, a polarization curve was then plotted for the respective voltage readings. The

peak of the plotted polarization curve was examined as maximum power generated by the ML-MFC.

### 3.5.6. Biomass Determination of *Bacillus subtilis* (BS)

The presence of BS in the ML-MFC system was determined in this study by identifying the availability of the bacteria within the system over the course of the seven-day incubation period according to the method described by Tranter (2016) [18], with slight modifications. In acquiring such data, a standard calibration curve of the biomass in the ML-MFC system was constructed prior to the incubation period based on the stock solution. In preparing the stock solution, a total mass of one gram sample (0.5 g dewatered sludge and 0.5 g chicken manure) was transferred into a one-liter volumetric flask and was diluted and topped up with deionized water. The stock solution was then utilized to construct the standard calibration curve (Appendices A and B) through further serial dilutions. An optical density approach was employed to monitor the turbidity of the sample through the use of a UV-vis spectrophotometer (HITACHI, model U-1900, Tokyo, Japan) with a 600 nm single light ray. Throughout the seven-day incubation period, a total mass of 1 gram of sample from the ML-MFC was collected and diluted with a total volume of 9 mL of deionized water in a 15 mL falcon tube. The absorbance readings (turbidity) of the sample were then monitored every twelve hours using a UV-vis spectrophotometer (HITACHI, model U-1900) with a 600 nm single light ray and deionized water as the blank. The acquired OD values (absorbance readings) were then interpreted as a standard unit (mg/L) of biomass with the standard calibration curve equation.

## 3.6. Fermentation Kinetics

The kinetic values of the ML-MFC system, such as the specific growth rate and doubling time, were calculated in order to obtain a microbially based observation. Specific growth rate ( $\mu$ ) can be defined as the rate at which the biomass population increases per unit of biomass concentration [19,20]

### 3.6.1. Specific Growth Rate ( $\mu$ ) of BS

Specific growth rate ( $\mu$ ) is an important kinetic value to calculate in a microbially related study, as it indirectly represents the dynamic behaviors of microbes within the system [19,21]. The value is calculated during the log phase of microbial development using the following equation (Appendix C):

$$\text{Specific growth rate, } \mu \left( \text{h}^{-1} \right) = \frac{\ln(X_{\text{Final}} - X_{\text{Initial}})}{\text{Total hours (h)}} \quad (1)$$

where  $\mu$  is the specific growth rate ( $\text{h}^{-1}$ ),  $X_{\text{Final}}$  is the final cell concentration (mg/L), and  $X_{\text{Initial}}$  is the initial cell concentration (mg/L)

### 3.6.2. Doubling Time ( $T_d$ ) of BS

Doubling time is the amount of time that is required by a micro-organism to double its population from the initial concentration [19,22,23] also known as the generation time. The doubling time values vary from one organism to another and from one condition to another, making it an important kinetic value to be calculated. In this study, the doubling time was calculated using the following formula (Appendix C):

$$\text{Doubling time, } T_d \text{ (h)} = \frac{\ln 2}{\mu} \quad (2)$$

## 4. Conclusions

According to this research, electricity can be generated utilizing ML-MFCs that are fueled by sludge supplemented with chicken manure. According to our analysis, the potential of such a system was found to be significant. Proximate analyses conducted on both

sludge and chicken manure identified carbon as the most abundant macronutrient component, accounting for 23.75% and 34.20% of the total composition, respectively. Magnesium accounted for the highest proportion of micronutrients for both sludge and chicken manure at 78.1575 mg/L and 71.6098 mg/L, respectively. The obtained COD values for dewatered sludge and chicken manure in this study were 708 mg/L and 571 mg/L, respectively. The obtained COD values were utilized as a standard value for the degradation of substrate by *Bacillus subtilis* in the ML-MFC system. Following optimization of parameter conditions (electrode distance, moisture content, and temperature) utilizing RSM (CCD), the maximum power density generated by the optimum ML-MFC was 47.2064 mW/m<sup>2</sup>, with a maximum biomass concentration of 19.6730 mg/L. The highest COD removal efficiency attained in this study was 98.0636%. The optimum parameter conditions for the operation of ML-MFC were determined to be 35 °C, 75% moisture content, and an electrode distance of 3 cm. The proposed optimal RSM parameter conditions of the ML-MFC system were verified, and we concluded that the ML-MFC's operating conditions can be optimized through the utilization of RSM via CCD. The acquired maximum power density, biomass concentration, and COD removal efficiency were 47.2064 mW/m<sup>2</sup>, 19.6730 mg/L, and 98.0636%, respectively. These values were determined to be within the range of 95% confidence level at 16.30–18.02 mg/L, 71.25–78.75%, and 34.44–38.06 mW/m<sup>2</sup>, respectively.

**Author Contributions:** Conceptualization, N.N.A.M., M.N.I.M.S., H.A.T. and M.M.Z.M.; supervision, H.A.T., N.F.S., H.S. and M.M.Z.M.; writing—original draft preparation, N.N.A.M. and M.N.I.M.S.; writing—review and editing, S.Z.A., Y.-C.Y. and M.R.; funding acquisition, M.M.Z.M. and M.R. All authors have read and agreed to the published version of the manuscript.

**Funding:** Ministry of Science and Technology (TDF08211437) and Higher Education Malaysia under the Fundamental Research Grant Scheme (FRGS/1/2019/STG05/USM/02/18).

**Data Availability Statement:** The data that support the findings of this study are available from the corresponding author upon reasonable request.

**Conflicts of Interest:** The authors declare no conflict to interest.

## Appendix A

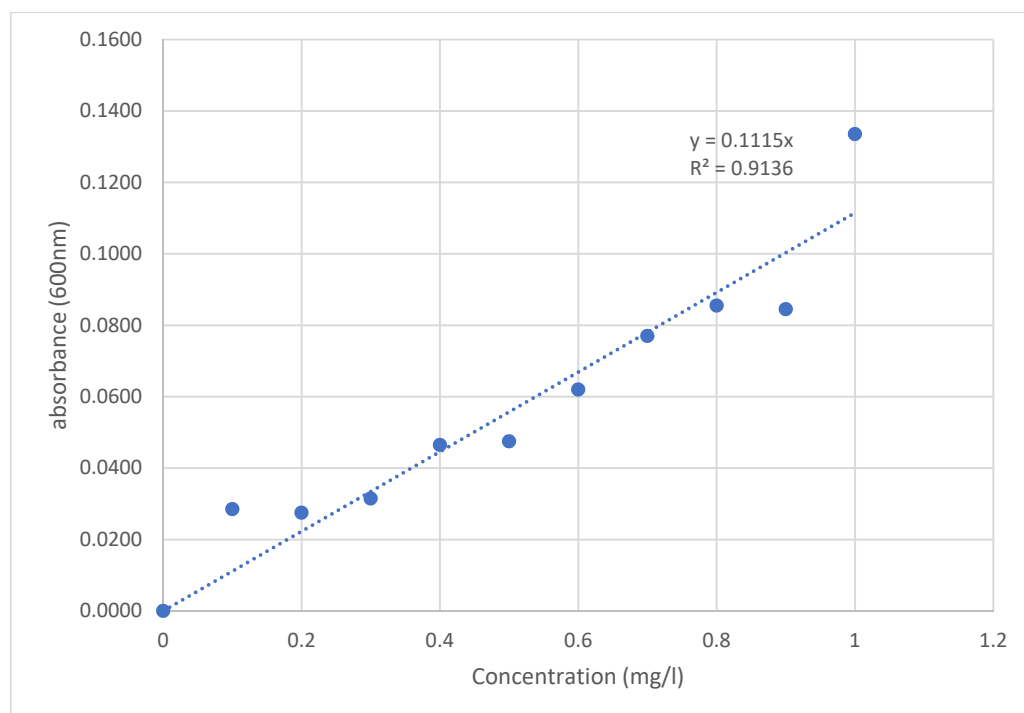


**Figure A1.** Standard calibration curve of chicken manure.



## Appendix B

A standard calibration curve (Appendix A) was used to translate the observed optical density (Abs) values into standard concentration units (mg/L).

$$y = 0.1115x$$

where y = optical density (Abs), and x = cell concentration (mg/L).

$$y = 0.1115 x$$

$$0.086 = 0.1115 x$$

$$x = 0.8 \text{ mg/L}$$

## Appendix C

Calculation of specific growth rate ( $\mu$ ) and doubling time ( $T_d$ ) for BS growth in raw broth in a shake flask (mimic ML-MFC):

$$\begin{aligned} \mu &= \frac{(\ln N_1 - \ln N_0)}{t_0 - t_1} \\ &= \frac{\ln(0.86996) - \ln(0.55157)}{6 - 2} \\ &= 0.113918 \text{ h}^{-1} \\ T_d &= \frac{\ln 2}{\mu} \\ &= 6.084591 \text{ h} \end{aligned}$$

## References

- Hinrichs, R.A.; Kleinbach, M.H. *Energy: Its Use and the Environment*, 5th ed.; Cengage Learnin: Boston, MA, USA, 2012; ISBN 978-1111990831.
- Panwar, N.L.; Kaushik, S.C.; Kothari, S. Role of renewable energy sources in environmental protection: A review. *Renew. Sustain. Energy Rev.* **2011**, *15*, 1513–1524. [CrossRef]
- Haiges, R.; Wang, Y.D.; Ghoshray, A.; Roskilly, A.P. Optimization of Malaysia's power generation mix to meet the electricity demand by 2050. *Energy Procedia* **2017**, *142*, 2844–2851. [CrossRef]
- Mekhilef, S.; Safari, A.; Mustafa, W.E.S.; Saidur, R.; Omar, R.; Younis, M.A.A. Solar energy in Malaysia: Current state and prospects. *Renew. Sustain. Energy Rev.* **2012**, *16*, 386–396. [CrossRef]
- Husain, Z.; Zainal, Z.A.; Abdullah, M.Z. Analysis of biomass-residue-based cogeneration system in palm oil mills. *Biomass Bioenergy* **2003**, *24*, 117–124. [CrossRef]
- Hirschmann, R. Malaysia: Poultry Consumption per Capita 2019. 2019. Available online: <https://www.statista.com/statistics/756920/malaysia-meat-consumption-per-capita-by-type/> (accessed on 1 July 2021).
- Department of Veterinary Services Malaysia (DVS). Guidelines for The Management of Pig Waste. Veterinary Malaysia. 2019. Available online: [https://www.dvs.gov.my/dvs/resources/user\\_1/2022/BPV/GP-Pengurusan-Sisa-Babi.pdf](https://www.dvs.gov.my/dvs/resources/user_1/2022/BPV/GP-Pengurusan-Sisa-Babi.pdf) (accessed on 1 July 2021).
- Hanum, F.; Yuan, L.C.; Kamahara, H.; Aziz, H.A.; Atsuta, Y.; Yamada, T.; Daimon, H. Treatment of sewage sludge using anaerobic digestion in Malaysia: Current state and challenges. *Front. Energy Res.* **2019**, *7*, 19. [CrossRef]
- Zahedi, S.; Martín, C.; Solera, R.; Pérez, M. Evaluating the Effectiveness of Adding Chicken Manure in the Anaerobic Mesophilic Codigestion of Sewage Sludge and Wine Distillery Wastewater: Kinetic Modeling and Economic Approach. *Energy Fuels* **2020**, *34*, 12626–12633. [CrossRef]
- Jaeel, A.J. Electricity Production from Dual Chambers Microbial Fuel Cell Fed with Chicken Manure-Wastewater. *Wasit J. Eng. Sci.* **2015**, *3*, 9–18. [CrossRef]
- El-Nahhal, Y.Z.; Al-Agha, M.R.; El-Nahhal, I.Y.; El Aila, N.A.; El-Nahal, F.I.; Alhalabi, R.A. Electricity generation from animal manure. *Biomass Bioenergy* **2020**, *136*, 105531. [CrossRef]
- Logan, B.E.; Harnelers, B.; Rozendal, R.; Schröder, U.; Keller, J.; Freguia, S. Microbial fuel cells: Methodology and technology. *Environ. Sci. Technol.* **2006**, *40*, 5181–5192. [CrossRef] [PubMed]
- Pandey, B.; Mishra, V.; Agrawal, S. Production of bio-electricity during wastewater treatment using a single chamber microbial fuel cell. *Int. J. Eng. Sci. Technol.* **2011**, *3*, 42–47. [CrossRef]
- Muaz, M.Z.M.; Abdul, R.; Vadivelu, V.M. Recovery of energy and simultaneous treatment of dewatered sludge using membrane-less microbial fuel cell. *Environ. Prog. Sustain. Energy* **2019**, *38*, 208–219. [CrossRef]
- Guangyin, Z.; Youcai, Z. Enhanced Sewage Sludge Dewaterability by Chemical Conditioning. In *Pollution Control and Resource Recovery: Sewage Sludge*; Elsevier Inc.: Amsterdam, The Netherlands, 2017; pp. 13–99. [CrossRef]

16. Logan, B.E.; Regan, J.M. Electricity-producing bacterial communities in microbial fuel cells. *Trends Microbiol.* **2006**, *14*, 512–518. [[CrossRef](#)] [[PubMed](#)]
17. Li, L.H.; Sun, Y.M.; Yuan, Z.H.; Kong, X.Y.; Li, Y. Effect of temperature change on power generation of microbial fuel cell. *Environ. Technol.* **2013**, *34*, 1929–1934. [[CrossRef](#)] [[PubMed](#)]
18. Tranter, J.; Crawford, K.; Richardson, J.; Schollar, J. Basic Practical Microbiology. In *Basic Practical Manual on Industrial Microbiology*; Lulu. com: London, UK, 2016; ISBN 0-95368-383-4.
19. Seok Oh, J.; Kim, B.G.; Hyun Park, T. Importance of specific growth rate for subtilisin expression in fed-batch cultivation of *Bacillus subtilis* spoIIIG mutant. *Enzyme Microb. Technol.* **2002**, *30*, 747–751. [[CrossRef](#)]
20. Smith, R.H. *Plant Tissue Culture*; Elsevier Inc.: Amsterdam, The Netherlands, 2013; ISBN 978-0-12-415920-4.
21. Sabri, M.N.I.M.; Shamsuddin, N.A.; Alias, M.F.A.; Tajaruddin, H.A.; Makhtar, M.Z. Assessment of Power Generation from Dewatered Sludge using Membrane-Less Microbial Fuel Cell. *IOP Conf. Ser. Earth Environ. Sci.* **2021**, *765*, 012060. [[CrossRef](#)]
22. Abbas, S.Z.; Rafatullah, M.; Khan, M.A.; Siddiqui, M.R. Bioremediation and Electricity Generation by Using Open and Closed Sediment Microbial Fuel Cells. *Front. Microbiol.* **2019**, *9*, 3348. [[CrossRef](#)] [[PubMed](#)]
23. Abbas, S.Z.; Rafatullah, M.; Ismail, N.; Shakoori, F.R. Electrochemistry and microbiology of microbial fuel cells treating marine sediments polluted with heavy metals. *RSC Adv.* **2018**, *8*, 18800–18813. [[CrossRef](#)] [[PubMed](#)]